Cantilever Dynamics using Small Amplitude AFM

A Thesis

submitted to
Indian Institute of Science Education and Research Pune
in partial fulfillment of the requirements for the
BS-MS Dual Degree Programme

by

Aadarsh Kumar

Indian Institute of Science Education and Research Pune
Dr. Homi Bhabha Road,
Pashan, Pune 411008, INDIA.

August 2021, 2021

Supervisor: Dr. Shivprasad Patil

Certificate

This is to certify that this dissertation entitled Cantilever Dynamics using Small Amplitude AFM towards the partial fulfilment of the BS-MS dual degree programme at the Indian Institute of Science Education and Research, Pune represents study/work carried out by Aadarsh Kumar at Indian Institute of Science Education and Research under the supervision of Dr. Shivprasad Patil, Associate Professor, Department of Physics , during the academic year 2020-2021.

Dr. Shivprasad Patil

Committee:

Dr. Shivprasad Patil

Dr. G.V. Pavan Kumar

This thesis is dedicated to my family, especially to my brother Deepak.

Declaration

I hereby declare that the matter embodied in the report entitled Cantilever Dynamics using Small Amplitude AFM are the results of the work carried out by me at the Department of Physics, Indian Institute of Science Education and Research, Pune, under the supervision of Dr. Shivprasad Patil and the same has not been submitted elsewhere for any other degree.

Aadarsh Kumar

Acknowledgments

I would like to thank my supervisor, Dr. Shivprasad Patil, for giving me the opportunity to work with him. I also thank him for his guidance and constant support throughout my research projects.

I express my sincere gratitude to my expert guide Dr. G.V. Pavan Kumar, for all the academic support. I want to thank him for evaluating my thesis work and the discussion and guidance he provided during my studies.

I am grateful to the institute(IISER Pune) for providing me with the resources, mainly for the experimental work. I also want to thank Dr. Ashna Bajpai for making my first lab experience great and for providing continuous support after that.

I would like to thank all of my lab members, especially Surya, Shatruhan, and Ajith, for making the lab a friendly environment to work in and for filling the tea breaks with some valuable discussion.

A special thanks to Surya for assisting me in designing the project and conducting the experiments. I also thank him for helping with all the academic and non-academic issues.

I would also like to acknowledge Shatruhan for all the detailed explanations of every academic and non-academic question I asked him, and also for giving me honest and valuable advice about what he learned through his life.

Last but not least, I thank all my friends and family for providing me the emotional support and encouragement throughout this academic journey.

Abstract

The dynamic force mode of spectroscopy measurements on the single molecules using soft cantilevers makes the bending signal easy to detect. But, there are many problems associated with soft cantilevers.

The aim and the results of this report are focused on one of the major sources of error when working with a soft cantilever in the dynamic mode of force spectroscopy at the off-resonance frequencies. When the stiffness of the cantilever and the derivative of the tip-sample interaction force are of the same order then, the solution of the cantilever dynamics becomes anharmonic.

Here, to present the anharmonicity in a quantitative manner, I have shown that the power present at drive frequency gets transferred to the higher harmonics during force mapping on single molecules. In this report, the power present at 2^{nd} harmonics has been investigated by demodulating the output signal and then sent to two lock-in amplifiers. The experiment was also performed in MATLAB and COMSOL software by creating a virtual environment. The output results agree with the statement made by the experimental results, which suggests to avoid use of a soft cantilever for the dynamic mode of force spectroscopy.

Contents

Abstract **xi**

1 Instrumentation **5**

2 Atomic Force Microscopy **7**

2.1 Modes of AFM 7

2.2 Small Amplitude AFM [1] 9

2.3 Cantilever Dynamics 10

2.4 Worm-Like Chain (WLC) Model [2] 13

3 Results and Discussion **15**

3.1 Computational Work(a) 15

3.2 Experiments 19

3.3 Computational Work(b) 26

4 Summary and Discussion **31**

Introduction

In recent years, scanning probe microscopy(SPM) has become a widespread and powerful technique. It is used in interdisciplinary fields like biophysics, material science, chemistry, soft matter, microelectronics, etc. The primary application of this instrument includes the electrical, rheological, topographical, and other mechanical properties of biomolecules and materials.

The first instrument of the SPM family, scanning tunneling microscopy(STM), was invented by Gerd Binning and Heinrich Rohrer at IBM Zurich in 1981. STM is used to study the electrical properties of conducting surfaces, but the working principles of SPM suggest that it is not suitable for non-conducting surfaces. In 1986 Binning, Quate, and Gerber invented atomic force microscopy to expand the types of surfaces on which atomic-scale information can be obtained[3].

Since its invention, AFM has become a fundamental technique for the nanoscale imaging of surfaces[4]. At first it was mostly used to characterize the non-biological material[5], [6]. Due to its capability to work in aqueous medium and room temperature, it became easy to study the biological sample in their functional and physiological environments. Therefore, shortly it was widely accepted by biophysicist[7]. The AFM is suitable to study the variety of biological matters, including biomolecules, biomaterials, cells, and tissues[8, 9, 10] .

AFM uses a sharp tip attached to a cantilever to probe the surface of the sample. The interaction force between the tip and the sample bends the cantilever. The detected signal of the bending of the cantilever tells us the properties of the sample.
The development of the new instrument, modification in the old concepts, building a theoret-

ical model with a minimal approximation is an exciting field for nanomechanics researchers. In 2005, Shivprasad Patil and Peter Hoffmann designed a Interferrometer based AFM(also called as Small Amplitude AFM)[11], which can be operated in liquid medium. And using an interferometer-based detection scheme in the instrument had provided it a sensitivity up to subangstrom level.

Due to the access of a highly sensitive instrument, I was able to design my experiment. My project makes a statement about the problems associated with using a soft cantilever in the dynamic mode of AFM at off-resonance frequencies.
The project involves understanding the dynamics of a cantilever dithered in a liquid environment; at a frequency that is far below its resonance. After that, use the home-built instrument; explicitly constructed to operate at these experimental conditions - 'Small amplitude Atomic Force Microscopy(SAAFM)[11]; to perform measurements on single macromolecules.

Stiffer cantilevers are advantageous on several levels, e.g., rigid cantilevers have lower thermal fluctuation amplitude, which will give more resolved signals. For off-resonance conditions - where the inertial and damping effects on the lever's dynamics can be neglected - the lever's resonance should be very high compared to the operating frequency; this is achieved easily by keeping the cantilever's stiffness high. Another major advantage is that it ensures the second derivative of the interaction potential (interaction stiffness) to be small as compared to cantilever stiffness; this criterion ensures the lever deflection to be a harmonic function at the operation frequency, implying that the interaction can be considered as a perturbation to the simple off-resonance dynamics of the cantilever. The only shortcoming of using stiff levers in the off-resonance condition is that their bending (inertial effects and damping) is negligibly small. The advantages as mentioned above become immensely crucial in a liquid environment - where almost all force spectroscopy experiments on biological molecules are done.

Since the commercial AFMs measure cantilever bending via optical lever deflection technique from the cantilever back, cantilevers of stiffness comparable or almost equal to the sample are used to get detectable bending amplitude. However, with the SAAFM, this shortcoming can be bypassed. The fundamental difference between commercial AFM and

SAAFM is that SAAFM measures cantilever displacement in the lab frame instead of the cantilever bending from its equilibrium position. This allows us to work even in off-resonance conditions with all the benefits associated with stiff cantilevers. The instrument measures the tip's displacement and incorporates an interferometer to measure displacements (higher sensitivity than commercial AFM); we get a better signal-to-noise ratio allowing us to detect sub-angstrom level drops in cantilever amplitude due to the sample interaction. Further, we can dither the cantilever with Angstrom level amplitudes, which are essential to probe the sample's energy landscape locally. Thus, the off-resonance operation and ultra-small amplitudes aid in the accurate reconstruction of the conservative and dissipative with high precision.

The work was to use the cantilevers of different stiffness (cantilever's stiffness(k_c) >>sample's stiffness(K_i), $k_c = K_i$ and $k_c < K_i$) to quantify protein stiffness. The expectations for the case $k_c = K_i$ and $k_c < K_i$ were that, the cantilever tip oscillation becomes anharmonic and leads to errors in the protein's stiffness inferred from the experiments.

Here, in this report I have compared the results obtained from soft cantilever and stiff cantilever. First I performed these experiment computationally(MATLAB) and the output supports the hypothesis, then I have shown with the experimental data that the solution is becomes more anharmonicity with a soft lever. Final conclusion I can deduce from this is that the for the soft levers the tip's dynamic has become anharmonic which can be quantified by measuring the power present at the second harmonic. and using a cantilever of stiffness>> sample's stiffness is advantageous.

Chapter 1

Instrumentation

For the force spectroscopy measurements, the cantilever is oscillated at fixed amplitude through piezo using alternating current, and the cantilever is bought towards sample(protein). When the tip touches the sample surface(coverslip), one end of the protein gets attached to the tip, and the other end was already attached to the coverslip. This situation is modeled similar to two connected springs. We detect bending in the cantilever when it retracts. When the restoring force of cantilever becomes more than the unfolding forces of proteins(sample), proteins unfold, and the cantilever comes back to zero bendings.

Commercial AFM vs SAAFM The primary components of both AFMs are illustrated in Figure 1.1 and 1.2 . In Commercial AFM, a laser is passed at the tip's backside, which acts as a mirror, and light reflects and goes to the photodetector. Bending in the cantilever changes the position of the laser spot on the detector.
While SAAFM works on interferometer-based detection schemes. An optical fiber (partially reflective at the end cross-section) is placed just above the cantilever's tip. When light is passed through the fiber, some fraction of the light reflects and goes to the detector, and the rest goes to the tip's back and reflects. We see a Fabry–Pérot interferometer cavity between fiber and the back of the tip; whenever there is a change in the relative distance, the interference pattern changes, and we detect this signal. And the next basic operations are the same as commercial AFM; cantilever touches the sample surfaces. It retracts, but here we directly detect the change in the tip position, unlike commercial AFM, where we probe the cantilever's bending.

We want to quantify the sample's stiffness during force spectroscopy for the extension in it. Commercial AFM detects the bending in cantilever, and SAAFM displays the change in the tip position. This fundamental difference makes the SAAFM more sensitive and accurate because, in SAAFM, we directly measure the change in length of the sample, while in commercial AFM, we subtract the measured quantity from the drive amplitude. Therefore we get a better signal-to-noise ratio with SAAFM and can easily operate even with a stiff cantilever.

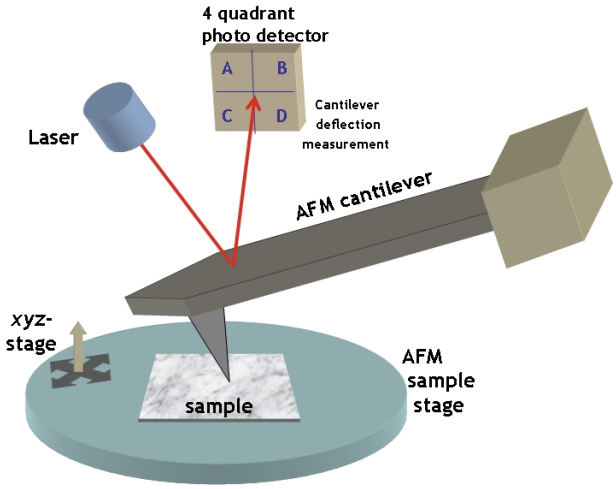

Figure 1.1: Schematic Representation of Commercial AFM with the name of its principle components(a)

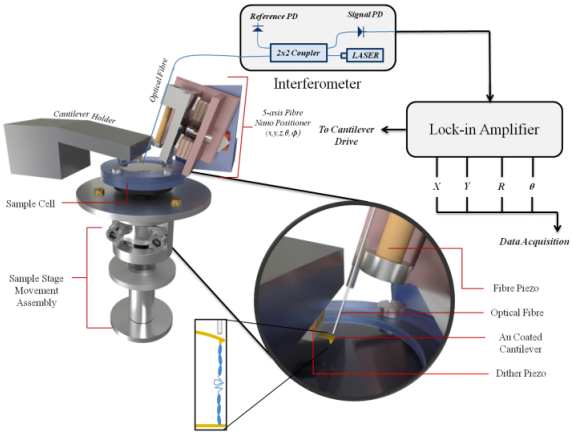

Figure 1.2: Schematic Diagram of the Home-Built Small Amplitude AFM

Chapter 2

Atomic Force Microscopy

This chapter includes the theoretical background we need to know for this experiment. Here I have tried to explain what AFM is and how it works, the assumption and mathematical models I used for analysis, and a concise introduction and mathematical form of polymer physics.

2.1 Modes of AFM

Atomic force microscopy has three common operational modes: **contact mode, tapping mode,** and **non-contact mode**.

The **contact mode** of AFM is also called static mode. Static mode is the simplest mode to operate an AFM among all three. In the contact mode of AFM, the tip scans through the sample while constantly being in contact with the sample surface. The interaction force and the topographical patterns affect the orientation of the tip and cantilever deforms. Information on the surface topography of the sample is gained from the feedback signal coming from the cantilever. In the static mode, the deflection of the cantilever(x) and the tip-surface interaction force(F_{ts}) are related by the formula, $x = F_{ts}/k$, where k is the stiffness of the cantilever.

Contact mode is not suitable for every type of sample. The tip-surface interaction force in the Z-direction and the shear force due to the lateral scan movement in the XY-plane could

induce deformation in the sample. One of the disadvantages of the contact mode is shown in a paper by Karrasch et al.[12], which says that if the sample is not absorbed to a solid surface, then it can easily be displaced during scanning, and that will reduce the resolution of the image. To overcome this fear, the tapping mode of AFM came into the picture[13, 14, 15, 16].

Dynamic mode of AFM can be performed in two different ways, tapping mode and non-contact mode. In the dynamic mode of operation, we oscillate the cantilever sinusoidally at a specified frequency and fixed amplitude. In the tapping mode, the tip lightly "taps" on the sample surface during each oscillation, contacting the surface at the bottom of its swing. The operational frequency in tapping mode is close to the resonance frequency, and the amplitude of oscillations is typically 20nm to 100nm, unlike non-contact mode, where the tip oscillates with a smaller amplitude($< 5nm$). The distance between tip and sample is one factor that differentiates the non-contact and intermittent contact mode(tapping mode). In the non-contact mode, the operation is performed in the attractive regime, while in tapping mode, the oscillation amplitude is large enough to overcome this attraction force. There are other factors such as radius of the tip, cantilever's stiffness, surface energy which affects the operational regimes. Therefore, oscillation amplitude is not enough to separate these two modes with a solid line.

A different and more straightforward way to divide the dynamic mode is Amplitude modulation AFM and Frequency Modulation AFM[17, 18].

Amplitude Modulation Atomic Force Microscopy(AM-AFM)

In the Amplitude modulation, cantilever is driven a vibrated at a fixed amplitude and specified frequency. When tip approaches the sample surface, tip-sample interaction($F_{ts}(z)$) influences the oscillation amplitude and phase(relative to the drive frequency). Drop in amplitude signals are used to determine the of the tip-sample interaction force, stiffness of sample and the change in phase has a correlation with the energy dissipation of sample. [1]

Frequency Modulation Atomic Force Microscopy(FM-AFM)

Another basic method of the dynamic mode is frequency modulation, here oscillating cantilever at resonance frequency changes the oscillator frequency due to the interaction force

[1] All the experiments were performed in Amplitude Modulation AFM mode

between tip and sample($F_{ts}(z)$). Using a frequency demodulating system, measure the change in resonance frequency which is a function of gradient of the interaction force($\frac{\partial F_{ts}(z)}{\partial z}$).

2.2 Small Amplitude AFM[1]

After the invention of SPM, there has been a development of many tools with similar working principles. With an ultimate goal to make the system more sensitive, less noisy, and more accurate, expanding the application, the modification and development of this instrument have never slowed down. The application of SPM is wide, and it's increasing with the development of the tool. For example, STM was not useful for imaging if non-conducting materials, but the invention of AFM solved this issue. Since AFM can work even in a liquid medium, biology provides several unexplored and exciting topics to explore. In the direction of probing the mechanical properties of biomolecules, a highly sensitive and interferometer-based atomic force microscopy was designed by S. Patil and P. Hoffmann[11].

The output signal of amplitude change tells us the stiffness of the single-molecule. The phase response of the cantilever is a dissipative signal, and it is used to draw the energy landscape of that molecule.

The interferometer-based AFM has proven itself more beneficial for the dynamic mode of force spectroscopy measurements than commercially available AFMs. Interferometer-based AFM is more sensitive, provides a better signal-to-noise ratio, and produces more accurate results than commercial AFM. The reason for detecting even a weak signal lies in the working principle concept, which is related to the fundamental differences in the signal detection system shown in Chapter 1.

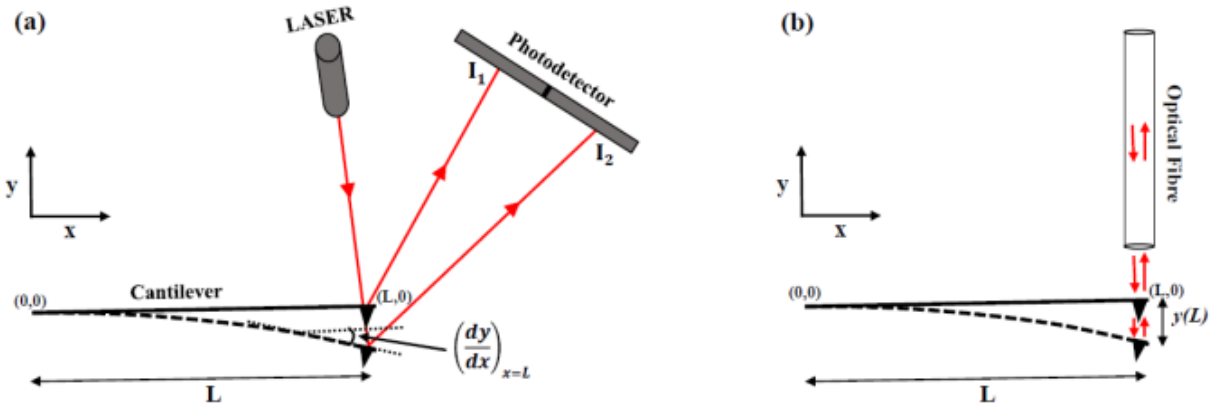

Figure 2.1: Left image and right shows the schematic diagram of major components of commercial AFM and SAAFM respectively. Left-down image nicely shows that commercial AFM measures the slope($\frac{dy}{dx}$) of the cantilever's bending at tip position and right-down image measures the displacement of tip(y)[8]

.

2.3 Cantilever Dynamics

Theory of Amplitude Modulation AFM

For the sinusoidal oscillation of a cantilever, the most common models which are used to describe the cantilever beam system are Point Mass Model and Continuous Mass Model.

2.3.1 Point Mass Model(PMM)

PMM is most simple and straightforward model to express cantilever numerical form. It assumes the cantilever as a point mass concentrated at the tip's position and that imaginary point mass oscillates with the same amplitude as tip. For the sinusoidal oscillation, PMM considers the potential of the system to be a harmonic, and the internal drag of lever or the drag forces of the medium(generally water or free space) acts as the the damping factors for the oscillation. Therefore, the dynamics of the tip's

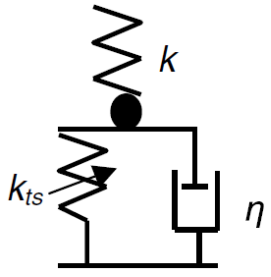

Figure 2.2: PMM representation of the system

position are solved using damped harmonic oscillator.[19]

$$m\ddot{z} = k_c z + \frac{m\omega_o}{Q}\dot{z} + F_o cos(\omega t) + F_{ts} \tag{2.1}$$

m-effective mass(m = 0.25m$_c$, m$_c$- mass of cantilever[19]), k_c- stiffness of the free cantilever, ω_o- natural frequency of cantilever, ω- driving angular frequency, F_o- drive force amplitude, F_{ts}- tip-sample interaction force, and d is the tip-sample separation

Solving for free cantilever, $\mathbf{F_{ts}(z) = 0}$

$$\omega_o = \sqrt{\frac{k}{m}} \tag{2.2}$$

$$A(\omega) = \frac{F_o/m}{[(\omega_o^2 - \omega^2)^2 + (\omega\omega_o/Q)^2]^{1/2}} \tag{2.3}$$

phase shift with respect to the drive signal

$$tan(\phi) = \frac{\omega\omega_o/Q}{\omega_o^2 - \omega^2} \tag{2.4}$$

Weakly perturbed harmonic oscillator($\mathbf{F_{ts}(z) \neq 0}$)
For small amplitude of oscillations, Taylor expansion for the interaction force can be approximated to the first order derivative,

$$F_{ts}(z) \approx F_{ts}(0) + \left.\frac{\partial F_{ts}}{\partial z}\right|_{z=0} z \tag{2.5}$$

Or,

$$F_{ts}(z) = F_{ts}(0) + k_{ts} z \tag{2.6}$$

where $k_{ts} = -(\partial F_{ts}/\partial d)_{z=0}$
By substituting F$_{ts}$ into equation 2.1,

$$m\ddot{z} = (k + k_{ts})z + \frac{m\omega_o}{Q}\dot{x} + F_o cos(\omega t) + F_{ts}(0) \tag{2.7}$$

If we write $k_{eff} = (k_c + k_{ts})$, then we realize it's nothing but a equation for the forced damped harmonic oscillator. After substituting k_c with k_{eff} in the solution of damped harmonic oscillator, we get

$$\omega_{eff} = \sqrt{\frac{k_{eff}}{m}} \tag{2.8}$$

$$\Delta\omega = \omega_{eff} - \omega_o$$

$$A(\omega) = \frac{F_o/m}{[(\omega_{eff}^2 - \omega^2)^2 + (\omega\omega_{eff}/Q)^2]^{1/2}} \tag{2.9}$$

For an off-resonance measurements of dynamic mode AFM,[1]

$$\omega << \omega_o$$
$$k_{ts} = k_c(\frac{A_o}{A}cos\phi - 1) \tag{2.10}$$

2.3.2 Continuous Mass Model(CMM)

Continuous mass model has less number of approximation than the point mass model. Continuous mass approximation is derived from the Euler-Bernoulli equation. Here, the geometry and boundary conditions of the cantilever are taken into consideration to solve the dynamics. This model provides a equation for the bending of a homogeneous rectangular cantilever. The key assumption is that the mass is distributed all along the length of the cantilever, unlike point mass model where mass is assumed to be centered at tip position. Modified Euler-Bernoulli Equation is used to express CMM in mathematical form.[19]

$$EI\frac{\partial^4}{\partial x^4}[w(x,t) + a_1\frac{\partial w(x,t)}{\partial t}] + \rho Wh\frac{\partial w^2(x,t)}{t^2} = -a_o\frac{\partial w(x,t)}{\partial t} + \partial(x-L)[F_{exc}(x,t) + F_{ts}(d)] \tag{2.11}$$

w(x, t)- time-dependent displacement of the cantilever in Z-direction at a point x in the X-direction, E-Young's modulus of cantilever, I-Area moment of inertia, a_1 = internal damping coefficient, a_o - external damping coefficient, h- thickness of the cantilever, L-length of the cantilever, W - width of the cantilever, ρ - mass density of the cantilever, F_{ext}(x, t)- excitation force, and F_{ts} - tip-surface interaction force

Using variable separation method to solve for w(x, t),
let's assume,

$$w(x,t) = X(x)Y(t)$$

For the case, when base is excited and there is no tip-surface interaction,
Vertical displacement at the base(clamped), X(0) = 0
Slope at the base(clamped), X'(0) = 0
Internal torque at the tip position(free end) in vertical direction, X"(L) = 0
Internal force at the tip position(free end) in the vertical direction, X"(L) = 0
Putting these boundary condition will give us discrete number of solution called eigenmodes. The general solution of the vertical displacement can be expressed in the superposition of the all the solutions[20].

$$w(x,t) = \sum_{i=1}^{n} X_n(x)Y_n(t) \tag{2.12}$$

Note

- For more detailed solutions, please follow the chapter 4 and 5 of the book "Amplitude Modulation Atomic Force Microscopy" written by Dr. Ricardo Garcia [19, 20]
  And please check the paper published by S. Rajput et al.[21], to know more about the recent development in these models. This paper compares the CMM and PMM; later, it also shows the optimum experimental conditions required for PMM approximation.
- The operational mode of the Small Amplitude AFM is amplitude modulation. Since here the tip's displacement is measured, the point-mass model provides a good approximation. And therefore, I used PMM for analysis; therefore, the theory section focuses on the point mass model and amplitude modulation of AFM.

2.4 Worm-Like Chain (WLC) Model[2]

The worm Like Chain(WLC) model translates the extensions in the polymers length into the force. It describes polymers' behavior with an assumption that polymers are a continuous flexible isotropic rod. The numerical form to calculate the restoring force of a protein at an extension z is given by[2],

$$F = \frac{K_B T}{L_p}\left(\frac{1}{(1-\frac{z}{L_c})^2} + \frac{z}{L_c} - \frac{1}{4}\right) \tag{2.13}$$

(where F is the force restoring force by WLC, K_B is a Boltzman's constant, L_c and L_p are contour and persistence length of the polymer respectively, and T is the temperature)
Since proteins are polymers in which the monomers are natural amino acids, and they are attached by the amide bonds, the WLC model can be used to estimate the restoring force of a protein at some finite extension.

In the single-molecule force spectroscopy measurements using AFM, we hold the molecule from both ends and apply mechanical stress on the molecules. This technique is widely used to observe the unfolding events of proteins under stress. This method is also very suitable for studying the energy dissipation of polymers, which changes their conformation under stress.

The sample of interest for me was Titin-I27 protein. Titin-I27 is a muscle protein whose main function is to act as a molecular spring in the contractile units in muscle cells. The mechanical behavior of this protein provides passive elasticity in muscles.

AFM is one of the very suitable instruments to study the mechanical unfolding events of Titin-I27 protein. Using AFM, the elastic properties and the energy profile of Titin-I27 protein under mechanical stress have already been shown in many papers. Since many people have already pointed out the basic properties of this protein, it was a good basis for my experiment to confirm the other parameters.

Chapter 3

Results and Discussion

3.1 Computational Work(a)

MATLAB For the first step of verification for my hypothesis, I used MATLAB software.
Here, I tried to replicate the experimental condition using equations in MATLAB. First, I oscillated the cantilever with an amplitude "A" at a fixed point in the z-direction and then added the WLC force at the tip position in -z-direction. Then, I solved the equation to get a time-dependent solution of the tip displacement. The equation was solved for two different cases- stiff cantilever and soft cantilever. The observed time-dependent solution was transformed into the Fourier space.

Figure 3.1: Point Mass Model Assumptions

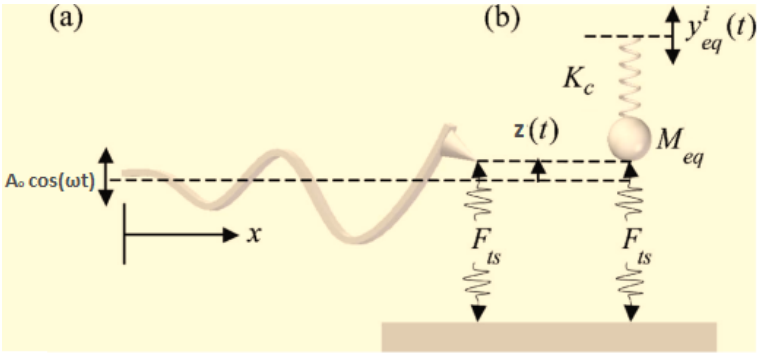

I used the point mass model to approximate the cantilever and the WLC model for the protein to solve the tip position dynamics. Figure 3.1 nicely illustrates the assumptions we make for point mass approximation. Cantilever is modeled as a linear spring for the small oscillation amplitude and the total mass is assumed to be placed at the tip's position.
I equated the force at tip position in z-direction. It can be easily visualised using Figure 3.1. The force at M_{eq} in the +z-direction is the restoring force of the cantilever due to bending. In the -z-direction, proteins pull M_{eq} downwards due to extension in it.

Since here the interaction force was represented by the WLC model, which is not linear, the motion of the tip was anharmonic.

$$k_c z + M_{eq}\gamma\dot{z} + M_{eq}\ddot{z} + F_{ts}(z) = M_{eq}\ddot{z}_o \tag{3.1}$$

Where k_c is the stiffness of a cantilever, z is the displacement of the tip in the z-direction, M_{eq} is the equivalent mass of a cantilever, z_o is a drive, and $\dot{z}$ & $\ddot{z}$ represent the first and second time derivative of z.

When a protein is attached to the tip, then the interaction force(F_{ts}(z)) between the tip and the sample can be modeled using WLC force. Equating the F_{ts}(z) with the WLC force equation and neglecting all the inertial terms in the equation will give-

$$k_c(A_o cos(\omega t) - d) = \frac{K_B T}{L_p}\left(\frac{1}{(1-\frac{d}{L_c})^2} + \frac{d}{L_c} - \frac{1}{4}\right) \tag{3.2}$$

In the dynamic mode of AFM, the lever gets data at a finite number of points in the z-direction, and at each point base of the lever oscillates sinusoidally for a specified time(time constant).

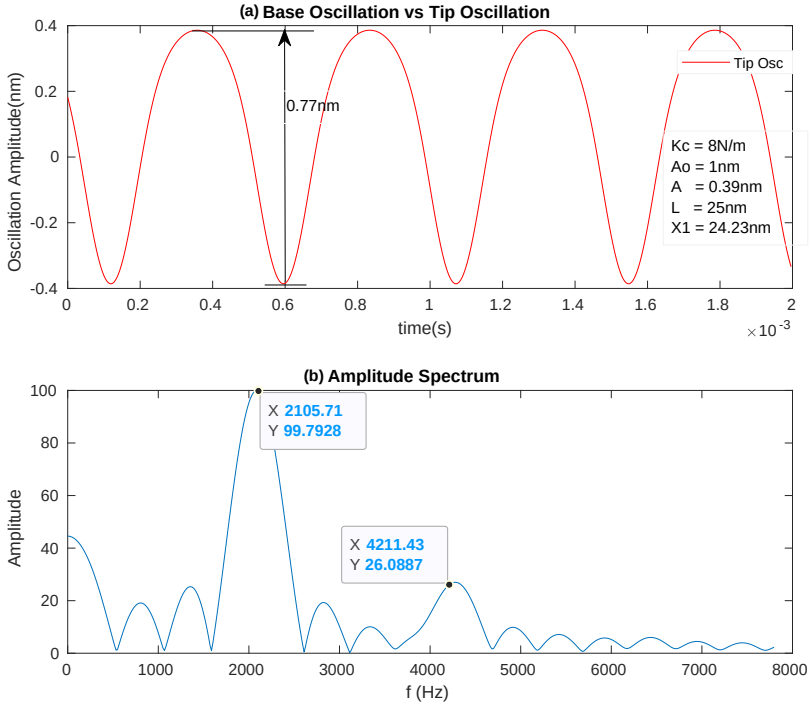

Figure 3.2: Stiff Cantilever($k_c = 8$N/m)
(a) Time domain(Time vs Oscillation Amplitude), (b) Frequency domain(Frequency vs Normalised Amplitude)

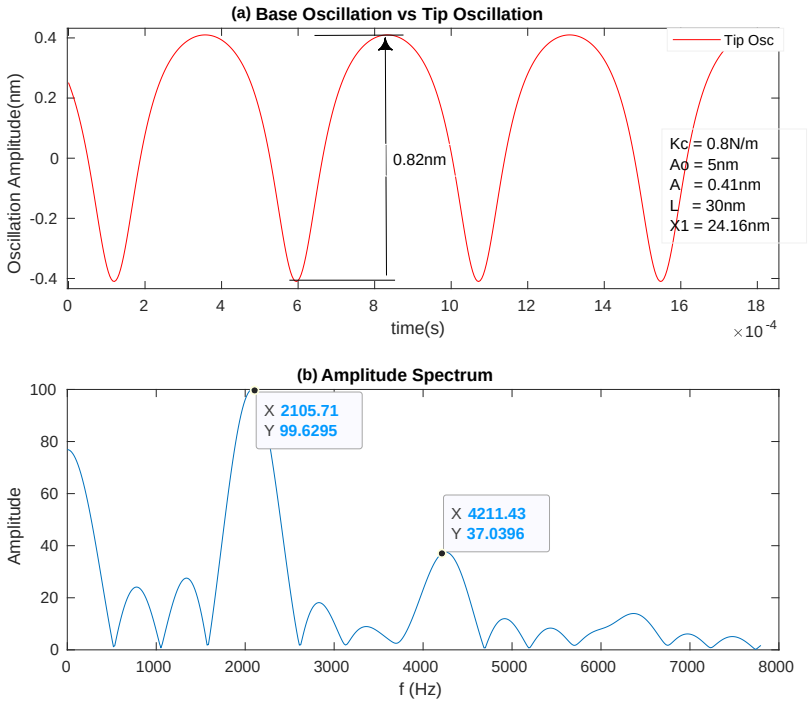

Figure 3.3: Soft Cantilever($k_c = 0.8$N/m)
(a) Time domain, (b) Frequency domain
In the frequency space, the higher of amplitude at second harmonics, more is the deviation of the from harmonicity.

The non-linear spring behavior of the WLC model is prominent when the extension in the sample is close to the contour length. I oscillated the cantilever at z $\approx$ 24 nm for a protein of contour length 25 nm. To get a first step confirmation of my hypothesis, I oscillated the cantilever at a point near the contour length so that the non-linearity is enough to make the signal anharmonic. Drive frequency(ω) for both the cantilever was 2.1 kHz.

Figure 3.2 is for cantilever of stiffness 8 N/m(stiff), and Figure 3.3 is for soft cantilever(80 mN/m). Figure 3.2 (a) and 3.3 (a) shows the tip position with respect to the time. And FIgure 3.2 (b) and 3.3 (b) are the Fourier transforms of their time domain signal, which is shown in 3.2 (a) and 3.3 (a). For the Fourier transformation, I used the FFT function in MATLAB.

Point Mass Model

$$\text{Sample's stiffness}(K) = k_c\left(\frac{A}{A_o}(1 - \frac{\omega^2}{\omega_o^2})^{-1}cos(\phi) - 1\right)$$

for off resonance condition, $\omega << \omega_o$ and $\phi \approx 0^o$

$$\text{Sample's stiffness}(K) = k_c(\frac{A_o}{A} - 1)$$

WLC stiffness[2.4],

$$K = \frac{dF(z)}{dz} = \frac{K_B T}{L_p}(\frac{2}{L_c(1-\frac{z}{L_c})^3} + \frac{1}{L_c}) \tag{3.3}$$

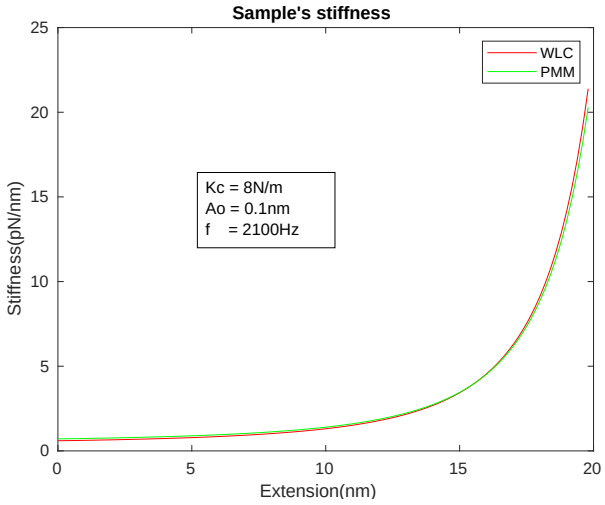

Figure 3.4: WLC prediction(red) and PMM approximated curve(green) for a Titin-I27 protein using a Stiff Cantilever($k_c = 8$N/m)

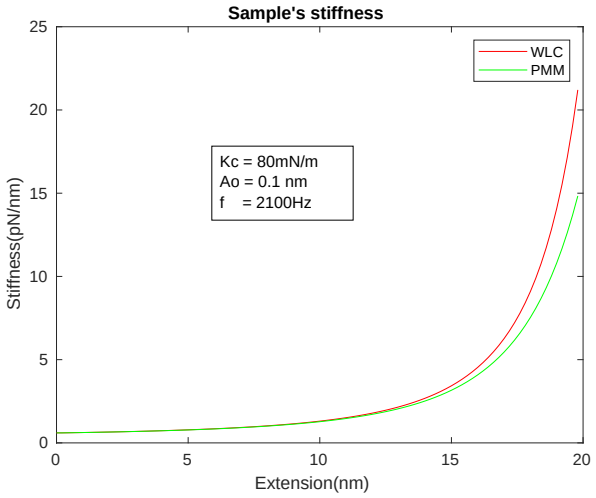

Figure 3.5: The separation of PMM(green) approximated curve from the WLC prediction(red) becomes prominent for the Soft Cantilever($k_c = 80$mN/m)

The above curves(Figure 3.4 and 3.5) has been plotted using point mass model approximation(blue) and using the WLC model(red). The time constant for the each data points were 30 ms, oscillation amplitude was $1\mathring{A}$ and the drive frequency was 2.1 kHz.

Discussion Let's look closely at the upper curves in both Figures 3.2 and 3.3. It is easy to observe that the output of the soft cantilever(Figure 3.3) is deviating from the sinusoidal nature more than the output signal of the stiff lever(Figure 3.2).
Transforming the same signal into frequency space has made it more clear. We can see that the normalized amplitude at second harmonics(4.2 kHz or 2ω) is more in the case of the soft cantilever(37 %) than the stiff cantilever(%26), which means the solution has become more anharmonic for a soft lever. In the case of the soft lever, we can also see a bump at the third harmonics(6.3 kHz).

In Figure 3.4, where the stiffness of the cantilever is 8N/m, the point mass model is nicely following the WLC model till the 20 nm of extension in a polymer. In contrast, under the same condition experimenting

with a soft cantilever(80 mN/m), I observed that the difference in WLC prediction from PMM is more in Figure 3.5.

3.2 Experiments

The results observed in the MATLAB(section 3.1)were enough to proceed for further steps. So, this section describes the next phase of the project, which was modifications with the instrument, experimental data, and analysis.

3.2.1 Instrumentation

As we see in Figure 3.3, the Fourier transform of the wave will tell us the anharmonicity of that signal. But, the SAAFM output signal is not the complete waveform, but it's the amplitude of the wave present at the drive frequency(ω).

With the aim to measure the power at the second harmonic, I used two Lock-in amplifiers for the measurement. And to install a secondary Lock-in Amplifier in the Small Amplitude AFM instruments, I modified the controlling program (coded in LabVIEW) as per the experimental requirements.

Lock-in Amplifier(LIA)[22] Lock-in Amplifier is an instrument that takes an input signal and returns the output signal with information for the specified frequency.

SAAFM uses an SR830 Lock-in Amplifier for the measurement of the amplitude. According to the manual of an SR830([22]), it measures the amplitude at the specified harmonics of the passed signal. So the default system(SAAFM) measures the amplitude of the output signal at the drive frequency(1^{st} harmonic of an input waveform).

To answer why I needed two Lock-in amplifiers, we must be aware of the question, what exactly does the Lock-in amplifier measure. And that has a been answered in the SR830 Lock-in Amplifier manual[22] using an example.
Let's say, if we pass an square wave through Lock-in with a frequency ω and the peak-to-peak amplitude 2V. We already know that a square wave is composed of multiple sine waves at multiples of the frequency ω. In a simple word, we can write a 2V peak-to-peak square wave as a summation of the sine waves.

$$S(t) = 1.273sin(\omega t) + 0.4244sin(3\omega t) + 0.2546sin(3\omega t) + ... \tag{3.4}$$

In that case, if the reference frequency is of the SR830 is defined to be ω, then the output signal will be $1.273sin(\omega t)$and not the peak to peak voltage of the signal(2V). Similarly, if the reference frequency is set to be 3ω then the measured signal is $0.4244sin(3\omega t)$, and so on. Here, the last statement clarifies that to measure the signal at two frequencies at the same time, we need two lock-in amplifiers.

LabVIEW(Laboratory Virtual Instrument Engineering Workbench) LabVIEW is software where you create a controlling program for instruments by connecting the icons of the instruments and the graphical notation of output values using wires. This controlling program is called a virtual instrument(VI). VI has three major components, front panel, block diagram, and icon connector.
The controlling program for the SAAFM has been designed using LabVIEW. Generally, measurements of SAAFM are performed using one Lock-in Amplifier, which measures the amplitude of the signal at drive frequency. My aim, the investigation of the second harmonic of the oscillating signal of the tip, needed two Lock-in Amplifiers instruments in the system. To install one more Lock-in Amplifier, first I made modified the VI. I used the Stanford Research 830 instrument driver package, changed the LabVIEW program by passing the output signal into two Lock-in Amplifiers. The physical connection for data transportation was made using General Purpose Interface Bus (GPIB) IEEE-488.2 interface.
The initial connection of the SAAFM before modification is shown in Figure 3.6. After installation of the second LIA, the instrument became like the schematic diagram shown in Figure 3.7 One of the LIA measured the amplitude of the output signal at the drive frequency(ω), and the other was installed to measure it at a different frequency (generally at 2ω or ω_o) for the same signal.

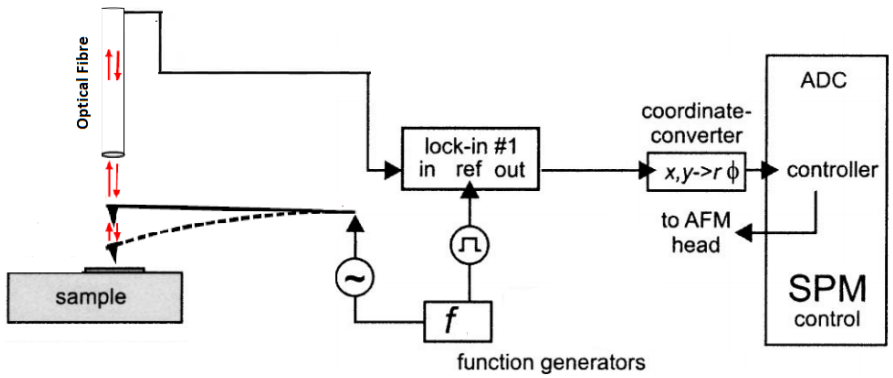

Figure 3.6: In general, the direction of data transfer takes place in the manner as shown in the above diagram

.

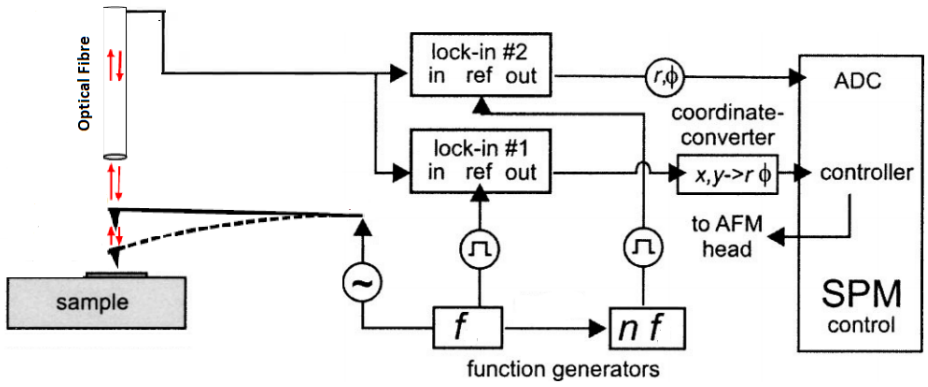

Figure 3.7: For this experiment, the output signal was divided in two signal and was going to the two LIAs instruments and both the LIAs was measuring amplitudes at the specified reference frequency.[23]

3.2.2 Materials and Methods

All the single molecule force spectroscopy experiments on Titin-I27 protein were performed using Interferometer based SAAFM protein. For the measurements, I used gold coated cantilevers of various dimensions and stiffness. One side of glass coverslips(sample surface) were coated with gold using thermal vapour deposition technique.

Cantilever's dimensions[1] : -

	Stiff Lever	**(a) Soft Lever** **(b) Soft Lever**
Dimensions(μm)	(300 ± 5) x (35 ± 3) x (2 ± 0.5)	(350 ± 5) * (32 ± 3) * (1 ± 0.5) (300 ± 5) * (32 ± 3) * (1 ± 0.5)
Stiffness (Measured)	1.268 N/m	85.46 mN/m 153 mN/m
Resonance Frequency (Measured)	21.68KHz	3.209 kHz 4.621 kHz

Table 3.1: Specification of the cantilevers

[1]All the cantilevers were bought from μmasch. The mentioned dimensions are taken from the specification brochure of the cantilever.

Procedure

- Do all the modifications with the instrument as suggested in section 3.2.1
- Get the gold-coated coverslips to put the sample on that, or get a glass coverslip and perform thermal vapour deposition of gold onto coverslips
- Attach the cantilever to the cantilever holder
- Place the coverslip on the sample stage
- Add 30μl of Titin-I27 protein on the coverslip and let the proteins bind to the gold surface for 30 minutes
- Gently rinse the sample surface 2-3 times with a buffer solution and then pour buffer into that such that cantilever can completely sink into that
- Fix the cantilever holder to the SAAFM system
- Turn on the system, and its operating software(SPM Nanomagnetics, Auto-Approach software, Data Acquisition Program, Frequency Sweep Program)
- Get the maximum sensitivity response of the system in SPM Nanomagnetics software by aligning the optical fiber at the back of the tip
- Bring the sample surface close to the cantilever, now cantilever and the lower cross-section of the optical fiber is dipped into the liquid medium
- Take a frequency scan of the cantilever using frequency sweep program, look for the off-resonance frequency where the system has a flat response
- Enter this frequency and other parameters in the Data Acquisition program
- Start the experiment
- Perform a soft analysis of the data in Grid-View Plot software and take the data of interest for further analysis

Make sure to note down the maximum sensitivity response, drive frequency, gain value of the system, and lock-in sensitivity after each set of experiments. They are needed for the analysis part, and the data filed formed in Data Acquisition software does not contain this information.

3.2.3 Experimental data

This section deals with the comparison of the output signal at the 2^{nd} harmonics of the drive frequency for the stiff cantilever and the soft cantilever.

For the force spectroscopy measurements two different kind of cantilevers were used stiff cantilever(k_c = 1.268 N/m) and soft cantilever(k_c = 0.08N/m).
The drive frequency(ω) for the k_c= 1.268 N/m was 2.1 kHz, the scanning range in the z-direction was 400 nm, and the free amplitude of the cantilever was 4.5 Åwith a slight variation in each set of data. The output signal was divided into two signals, one was sent to lock-in$_1$ which was measuring the amplitude at the 1^{st} harmonic(ω), and the other one was sent to lock-in$_2$ which was returning the amplitude value present at the 2^{nd} harmonic(2ω = 4200 kHz) at the same time. In Figure ??, the blue line represents the drop in amplitude(free amplitude of cantilever - amplitude present at ω in the output signal), and the orange line represents the amplitude present at 2ω of the same signal.

The main observation to note here that the power present at the 2^{nd} harmonic is very low compared to the power lost at the 1^{st} harmonic. Even if there is any correlation between these two signals, then the noise floor is very high, and it is difficult to establish any relation between them.

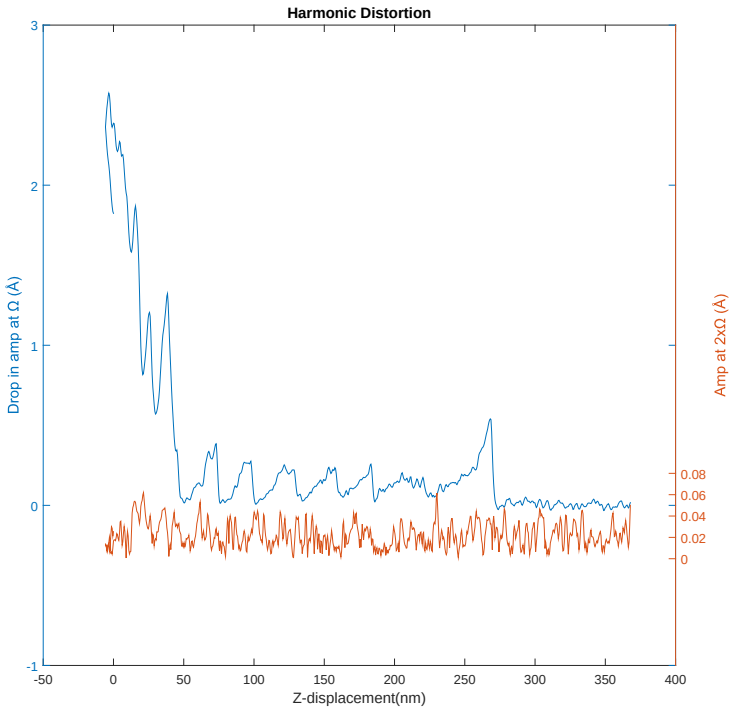

Figure 3.8: Stiff Cantilever: The amplitude signal at second(red) harmonic is lost inside the noise floor. Power transfer from the drive frequency (blue) to the second harmonics(red line) is very less.

The second half of the experiment was to perform the same experiment with a soft lever. I used a cantilever of stiffness 0.085 N/m. Here, the drive frequency was 400 Hz. The scanning range was the same as the previous one(400 nm). During the experiment, I tried to maintain other parameters the same as the stiff cantilever to avoid misinterpretation of data. Therefore free amplitude of the cantilever was 4.5Å. Both lock-ins were placed as before, and output data had the same meaning.
The data grabbed with a soft cantilever is shown in Figure 3.9. It is very clear from the top graph of Figure 3.9 that whenever there is a drop in amplitude at the drive frequency, then the fraction of the power is getting a transfer at the 2^{nd} harmonic. If we look closely, the rise in amplitude at 2ω is $\sim 20\%$ of the drop in amplitude at ω. The bottom part of the Figure shows us whenever we use a soft lever and quantify the stiffness of any sample using point mass model, we must be aware of the anharmonic nature of the tip's dynamics and the transferred power at frequencies other than the reference frequency.

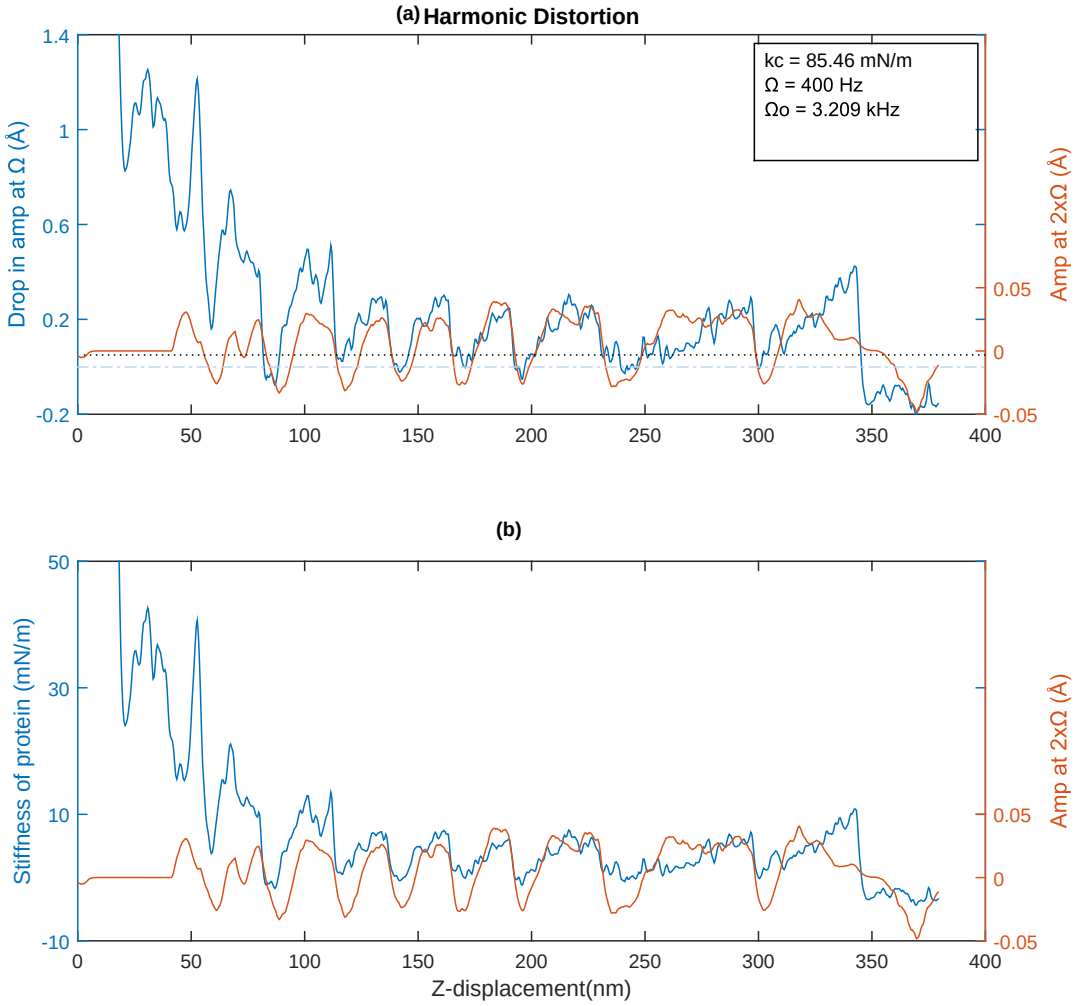

Figure 3.9: Soft Cantilever: (a) The correlation between the drop in amplitude at first harmonic(blue) and rise in amplitude at second harmonic(red) is clearly visible. (b) For each value of the stiffness of sample(blue), we neglect the power present at second or higher harmonics(red).

Observed Spectrum in Data The results mentioned above are some of the good curves I got in the experiment. But there are some other curves that neither provides any conclusive evidence and nor deny it. By only looking at them, it is hard to make any firm statement. Here, I am attaching some curves that do not stand at the extreme of a line of the perfect and disagreeable curve.

The experimental condition for the Figure 3.10 curve was the same as in the case of Figure 3.9. In this picture, the peaks of the curve for the 2^{nd} harmonic signal are definitely correlated with the drop in amplitude at ω. However, to make this statement bold, this signal is not sufficient in itself. At this point, when I already had some curves like Figure 3.9, then these curves are enough to provide support to my

claim.

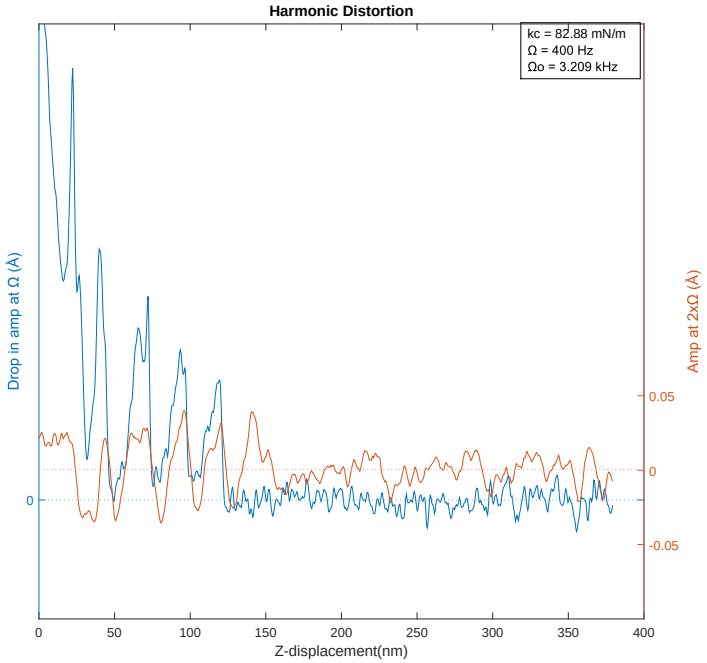

Figure 3.10: Soft Cantilever($k_c = 82.88$),
Noisy Data(a): For the first few unfolding domains, power lost at first harmonics(blue) and power gained at second harmonics(red) is correlated. But, after the protein detachment from the cantilever, the signal has become very noisy.

Due to the low amplitude measurements, few data sets didn't give a clear sign to make any precise statement. For e.x., some of the experiments were performed with a cantilever of the stiffness 153 mN/s. Figure 3.11 shows the amplitude present at the 1^{st} and 2^{nd} harmonic. The cantilever was driven at a 2.1 kHz frequency, and the oscillation amplitude and other parameters were similar to the rest of the previous experiments.

With the cantilever of stiffness 153 N/m, I couldn't see any signal at 2ω. But when I check it quantitatively, I noticed that the signal-to-noise ratio of the signal at 2ω is weak compared to the other cases. The width of the noise floor for the 2ω signal is $\sim 20\%$ of the drop in amplitude at the drive frequency when protein detaches. Even if there was some power transfer to the second harmonic, I couldn't see it due to noise. Therefore, I ignored these data by assuming a piece of inconclusive evidence.

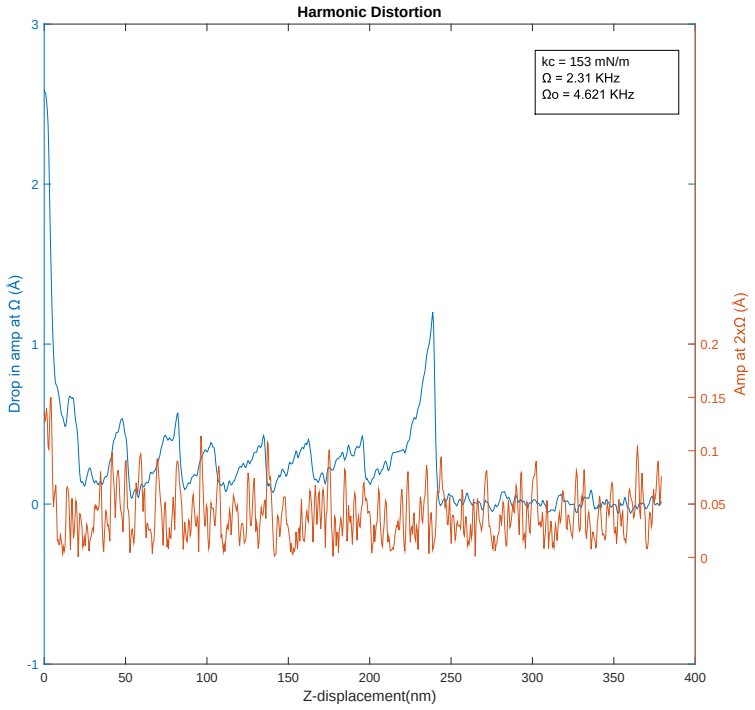

Figure 3.11: Soft Cantilever(k_c = 153 mN/m),
Noisy Data(b): The rise in amplitude signal at 2ω(red) is very noisy. The ratio of the width of the amplitude at second harmonics(noise floor width) is 20% of drop in amplitude at first harmonics(blue).

I also tried to perform the same experiment with the biolevers, but they too fragile for my experiments.

3.3 Computational Work(b)

3.3.1 COMSOL Multiphysics[24]

COMSOL Multiphysics is a software platform through which we can design our experiment in a virtual environment, and it simulates the experiment using available physics packages and our custom equations. The software simulates the experiment by breaking the system into multiple finite elements. It solves for each element separately and then gives us the results by merging all the results.

In the simulation performed in the MATLAB program, some approximations were made, like neglecting inertial terms, simulating vacuum medium. To add all the experimental conditions that I couldn't include

in MATLAB codes, to make a supporting argument for the obtained results in the last section(3.2.3), and to visualize my system more clearly, I modeled my experiment in the COMSOL Multiphysics software.
I used three multiphysics packages available in the COMSOL Multiphysics library. They are listed below.

1. Structural Mechanics(Solid Mechanics)
2. Fluid-Solid Interface(Laminar Flow)
3. Electrostatics(Piezoelectricity)

Designing the system in the virtual environment of COMSOL: -

- Selects the physics packages
- Select the study subjects

  Stationary - to calculate the stiffness,

  Eigenfrequency - to calculate resonance frequency, and

  time dependent - to solve for tip dynamics
- Define the dimension of the structures in "Geometry"

  Cantilever

  Chip of the cantilever(rigid material)

  Piezoelectric material

  sample cell
- Select the materials for each components in "Materials"

  Cantilever - Silicon

  Chip - Rigid material

  Piezoelectric Material - Lead Zirconate Titrate

  Sample Cell - Water
- Add physics
- Select the multiphysics interface
- create a mesh
- In the study section compute the results

The designed model is shown in Figure 3.12. The piezoelectric material is attached to a rigid material, and it does not deform when the piezo changes its shape due to expansion and compression.

The rigid material(chip) is connected to a long rectangular beam(cantilever). Cantilever and chip are dipped inside the water medium.

Figure 3.12: Cantilever Modeling in COMSOL

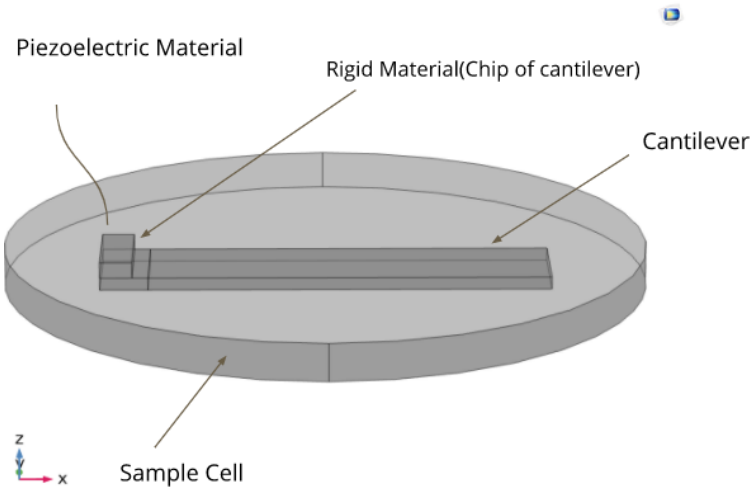

I passed an AC potential across the piezo in the vertical direction, and that causes it to expands and compresses sinusoidally. Due to that, the chip moves in the vertical direction, and so does the cantilever. The water medium provides the drag, almost similar to the real system.
(The flow cell in the experiment is an infinite bath, but due to computational load, I designed it slightly larger than the cantilever and ignored the reflection of the wave coming from the wall of the flow cell. Otherwise, In COMSOL, we have an option to design an infinite wall of a system, which could have been used as an infinite boundary wall.)

I designed two different kinds of the system, (a) a stiff cantilever and (b) a soft cantilever. The dimensions of each cantilever and its physical properties are mentioned in the Table 3.2

	(a) Stiff Lever	**(b) Soft Lever**
Dimension	$350 * 30 * 3\mu m$	$350 * 30 * 3\mu m$
Stiffness	0.95 N/m	71 mN/m
Eigenfrequency	36.73 KHz	10.07 kHz
Young's Modulus	200e9 GPa [25]	15e9 GPa

Table 3.2: Specification of the cantilevers

I had the freedom to define the cantilever's dimension and Young's modulus of the cantilever material. Generally, increasing the length and reducing the thickness make the beam softer. I also tried that, but for thin levers, I had to select the mesh size finest, and that increased the number of domains, and the computational time became very long. Another thing I tried was I entered the lower value of Young's modulus, which solved the problem. And since it wouldn't change much of the physics, the results should be approximately the same.

In Figure 3.13, the designs of cantilevers in COMSOL are shown. Natural frequency values are mentioned on the images, calculated using the eigenfrequency study from the COMSOL library. The stiffness mentioned in the 3.2 was calculated using Hooke's law of a linear spring by treating the bending of the cantilever as the extension in a spring. The next work is to apply the WLC force in the downward direction(-z) at a domain

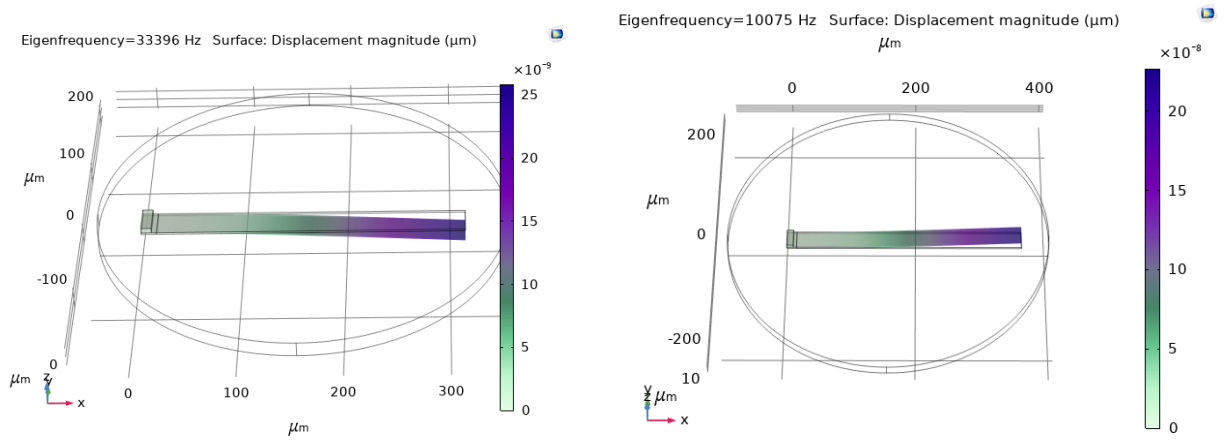

Figure 3.13: Cantilevers in virtual environment(COMSOL). Resonance frequency of the cantilever was calculated using the Eigenfreuency function in COMSOL. The resonance frequency of the stiff cantilever is 33.396 kHz, and for soft cantilever it is 10.075 kHz.

close to the tip position and then oscillate the system at a drive frequency(ω) by passing an AC across the piezo.

If WLC force is zero, the displacement of the point close to the tip region will be free oscillation amplitude. For non-zero WLC force, probing the displacement of the tip will be informative for the investigation of anharmonicity. The Fourier transform of the probe displacement curve will tell us if there is any signal present at the second harmonics(2ω).

Future plans and expectations: - My short-term goal is to complete the simulation in COMSOL. The output results in COMSOL will be an amplitude vs. time curve, similar to the curve shown in Figure 3.2 and 3.3. I have already simulated a similar experiment in a vacuum medium. In the vacuum medium, the excited eigenmodes take a long time to disappear. In water medium, the quality factor of the lever is low; therefore, the transient time will be short, and the system will reach equilibrium fast. In COMSOL simulation, less approximation has been made; therefore, the data will be more accurate and close to the actual experiment than the MATLAB simulation. Fourier transform of the amplitude vs. time curve will provide us a quantitative measure of the anharmonicity of the tip's dynamics. The power present at the higher harmonics in Fourier space will be used to calculate the "Total harmonic distortion."

Chapter 4

Summary and Discussion

After looking at the soft cantilever's advantages(such as the detectable signal even for the week forces, easy to work with less sensitive instruments) and disadvantages, it is advisable to avoid using soft cantilevers. And to make this statement clear in quantitative manner, here, I have presented the errors associated with the use of soft cantilevers.

For that, the first step verification was done in MATLAB simulation. In section 3.1, I have shown that the signal is deviating from sinusoidal nature more in the case of soft lever than stiff lever. The anharmonicity of the output signal increases to the shift between stiffness calculated using the WLC and PMM model.

After getting a first step verification from the MATLAB simulation results, I proceeded with the experiments. To measure the power dissipation at higher amplitudes, I installed one more lock-in amplifier to the SAAFM by modifying the controlling program of SAAFM(LabVIEW). And then, I performed experiments with the cantilevers of stiffness 8N/m and 85mN/m by keeping the drive frequency from the off-resonance frequency range and oscillation amplitude small.

The experimental section 3.2.3 confirms the hypothesis by showing similar results. The main observation here is that, for a cantilever of stiffness 85mN/m, the rise in amplitude at 2^{nd} harmonics(2ω) is about 20% of the drop in amplitude at 1^{st} harmonics. While in the case of a stiff lever(8N/m), the detected signal at frequency 2ω was so week that it is lost in the noise floor.

The conclusion we make from this work is that soft cantilevers are not suitable for force spectroscopy measurement at off-resonance frequencies. If we have to use a soft cantilever for an experiment, we must consider the power present at higher harmonics during analysis.

To provide a supportive argument, I am also performing the same experiment in COMSOL by creating a virtual environment. I will run the simulations for the three types of cantilevers, stiff cantilever, soft cantilever, and biolevers. And will compare the power dissipated at higher harmonics for each cases.

Bibliography

[1] S. Patil and P. Hoffmann, "Small-amplitude atomic force microscopy," *Advanced Engineering Materials*, vol. 7, no. 8, pp. 707–712, 2005. [Online]. Available: https://onlinelibrary.wiley.com/doi/abs/10.1002/adem.200500054

[2] J. N. Milstein and J.-C. Meiners, *Worm-Like Chain (WLC) Model*. Berlin, Heidelberg: Springer Berlin Heidelberg, 2013, pp. 2757–2760. [Online]. Available: https://doi.org/10.1007/978-3-642-16712-6_502

[3] G. Binnig, C. F. Quate, and C. Gerber, "Atomic force microscope," *Phys. Rev. Lett.*, vol. 56, pp. 930–933, Mar 1986. [Online]. Available: https://link.aps.org/doi/10.1103/PhysRevLett.56.930

[4] G. Binnig, C. Gerber, E. Stoll, T. R. Albrecht, and C. F. Quate, "Atomic resolution with atomic force microscope," *Europhysics Letters (EPL)*, vol. 3, no. 12, pp. 1281–1286, jun 1987. [Online]. Available: https://doi.org/10.1209/0295-5075/3/12/006

[5] O. Marti, B. Drake, and P. K. Hansma, "Atomic force microscopy of liquid-covered surfaces: Atomic resolution images," *Applied Physics Letters*, vol. 51, no. 7, pp. 484–486, 1987. [Online]. Available: https://doi.org/10.1063/1.98374

[6] T. Albrecht and C. Quate, "Atomic resolution imaging of a nonconductor by atomic force microscopy," *Journal of Applied Physics*, vol. 62, no. 7, pp. 2599–2602, 1987.

[7] S. Gould, O. Marti, B. Drake, L. Hellemans, C. E. Bracker, P. K. Hansma, N. L. Keder, M. M. Eddy, and G. D. Stucky, "Molecular resolution images of amino acid crystals with the atomic force microscope," *Nature*, vol. 332, no. 6162, pp. 332–334, 1988.

[8] S. Rajput, S. Deopa, J. Yadav, V. Ahlawat, S. Talele, and S. Patil, "The nano-scale viscoelasticity using atomic force microscopy in liquid environment," *Nanotechnology*, vol. 32, 10 2020.

[9] R. D. Mote, J. Yadav, S. B. Singh, M. Tiwari, S. Patil, D. Subramanyam *et al.*, "Pluripotency of embryonic stem cells lacking clathrin-mediated endocytosis cannot be rescued by restoring cellular stiffness," *Journal of Biological Chemistry*, vol. 295, no. 49, pp. 16 888–16 896, 2020.

[10] S. Naik, M. Unni, D. Sinha, S. Rajput, P. Chandramouli reddy, A. Chatterji, S. Patil, and S. Galande, "Differential tissue stiffness of body column facilitates locomotion of hydra on solid substrates," 03 2020.

[11] S. Patil, G. Matei, H. Dong, P. M. Hoffmann, M. Karaköse, and A. Oral, "A highly sensitive atomic force microscope for linear measurements of molecular forces in liquids," *Review of Scientific Instruments*, vol. 76, no. 10, p. 103705, 2005. [Online]. Available: https://doi.org/10.1063/1.2083147

[12] S. Karrasch, M. Dolder, F. Schabert, J. Ramsden, and A. Engel, "Covalent binding of biological samples to solid supports for scanning probe microscopy in buffer solution," *Biophysical journal*, vol. 65, no. 6, pp. 2437–2446, 1993.

[13] Q. Zhong, D. Inniss, K. Kjoller, and V. Elings, "Fractured polymer/silica fiber surface studied by tapping mode atomic force microscopy," *Surface Science*, vol. 290, no. 1, pp. L688–L692, 1993. [Online]. Available: https://www.sciencedirect.com/science/article/pii/0039602893905825

[14] C. A. J. Putman, K. O. Van der Werf, B. G. De Grooth, N. F. Van Hulst, and J. Greve, "Tapping mode atomic force microscopy in liquid," *Applied Physics Letters*, vol. 64, no. 18, pp. 2454–2456, 1994. [Online]. Available: https://doi.org/10.1063/1.111597

[15] P. K. Hansma, J. P. Cleveland, M. Radmacher, D. A. Walters, P. E. Hillner, M. Bezanilla, M. Fritz, D. Vie, H. G. Hansma, C. B. Prater, J. Massie, L. Fukunaga, J. Gurley, and V. Elings, "Tapping mode atomic force microscopy in liquids," *Applied Physics Letters*, vol. 64, no. 13, pp. 1738–1740, 1994. [Online]. Available: https://doi.org/10.1063/1.111795

[16] C. Möller, M. Allen, V. Elings, A. Engel, and D. J. Müller, "Tapping-mode atomic force microscopy produces faithful high-resolution images of protein surfaces," *Biophysical journal*, vol. 77, no. 2, pp. 1150–1158, 1999.

[17] F. J. Giessibl, "Advances in atomic force microscopy," *Rev. Mod. Phys.*, vol. 75, pp. 949–983, Jul 2003. [Online]. Available: https://link.aps.org/doi/10.1103/RevModPhys.75.949

[18] A. T.R., G. P., H. D., and R. D., "Frequency modulation detection using high-q cantilevers for enhanced force microscope sensitivity," *Journal of Applied Physics*, vol. 69, pp. 668–673, 1991. [Online]. Available: https://doi.org/10.1063/1.347347

[19] *Theory of Amplitude Modulation AFM.* John Wiley & Sons, Ltd, 2010, ch. 4, pp. 41–57. [Online]. Available: https://onlinelibrary.wiley.com/doi/abs/10.1002/9783527632183.ch4

[20] *Advanced Theory of Amplitude Modulation AFM.* John Wiley & Sons, Ltd, 2010, ch. 5, pp. 59–76. [Online]. Available: https://onlinelibrary.wiley.com/doi/abs/10.1002/9783527632183.ch5

[21] S. S. Rajput, S. P. S. Deopa, V. Ajith, S. C. Kamerkar, and S. V. Patil, "Validity of point-mass model in off-resonance dynamic atomic force microscopy," *Nanotechnology*, 2021.

[22] "Sr830 dsp lock-in amplifier," *Stanford Research System*. [Online]. Available: https://www.thinksrs.com/downloads/pdfs/manuals/SR830m.pdf

[23] R. W. Stark and W. M. Heckl, "Higher harmonics imaging in tapping-mode atomic-force microscopy," *Review of Scientific Instruments*, vol. 74, no. 12, pp. 5111–5114, 2003. [Online]. Available: https://doi.org/10.1063/1.1626008

[24] "Comsol multiphysics." [Online]. Available: https://doc.comsol.com/5.5/doc/com.comsol.help.comsol/COMSOL_ReferenceManual.pdf

[25] K. Petersen, "Silicon as a mechanical material. proc. ieee. 70," 1982.